Electronic Supplementary Information

A Facile Route to Synthesize Multiporous $MnCo_2O_4$ and $CoMn_2O_4$ Spinel Quasi-Hollow Spheres with Improved Lithium Storage Properties

Jingfa Li, Shenglin Xiong,* Xiaowei Li, and Yitai Qian

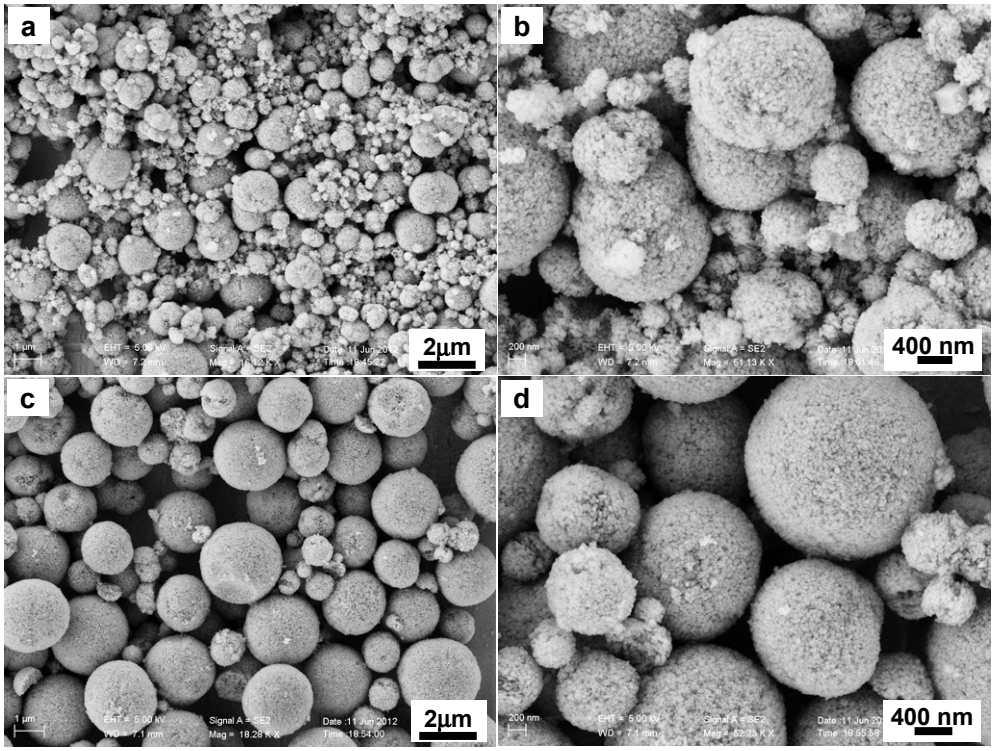

Figure S1. Low and high magnification FESEM images of the $Mn_{0.33}Co_{0.67}CO_3$ (a,b) and $Co_{0.33}Mn_{0.67}CO_3$ (c,d) precursors synthesized in distilled water at 200 °C for 20 h.

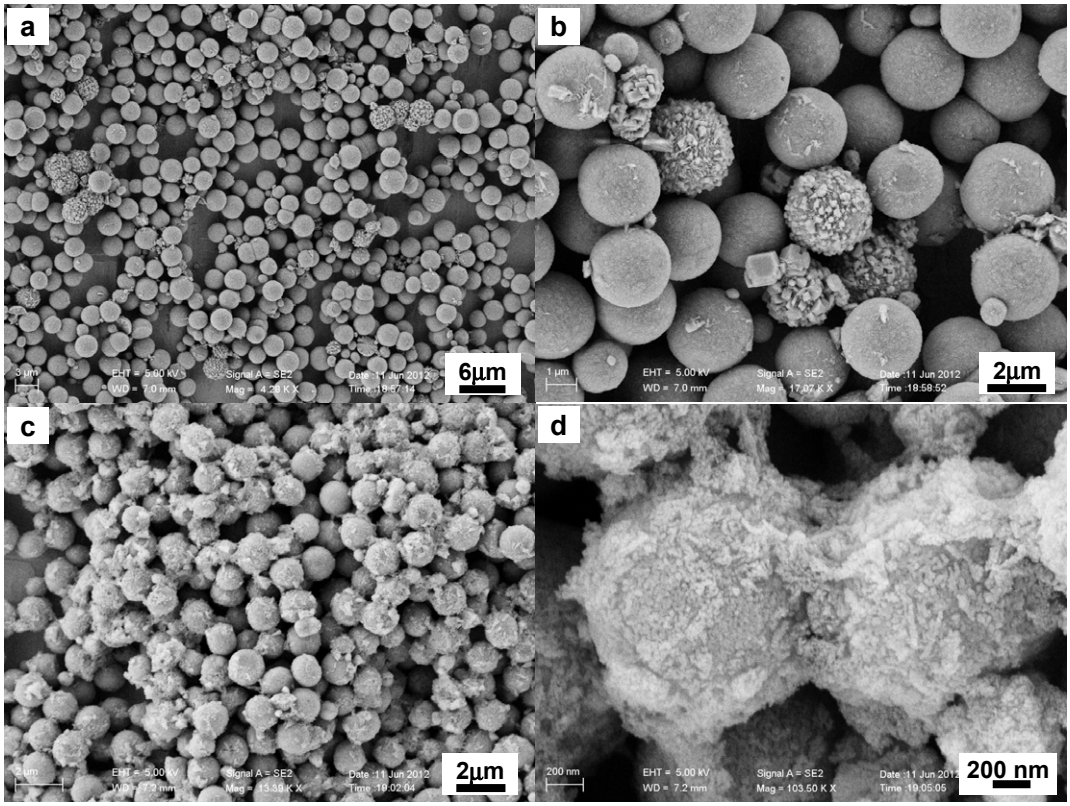

Figure S2. Low and high magnification FESEM images of the $Mn_{0.33}Co_{0.67}CO_3$ (a,b) and $Co_{0.33}Mn_{0.67}CO_3$ (c,d) precursors synthesized solvothermally at 180 °C for 20 h.

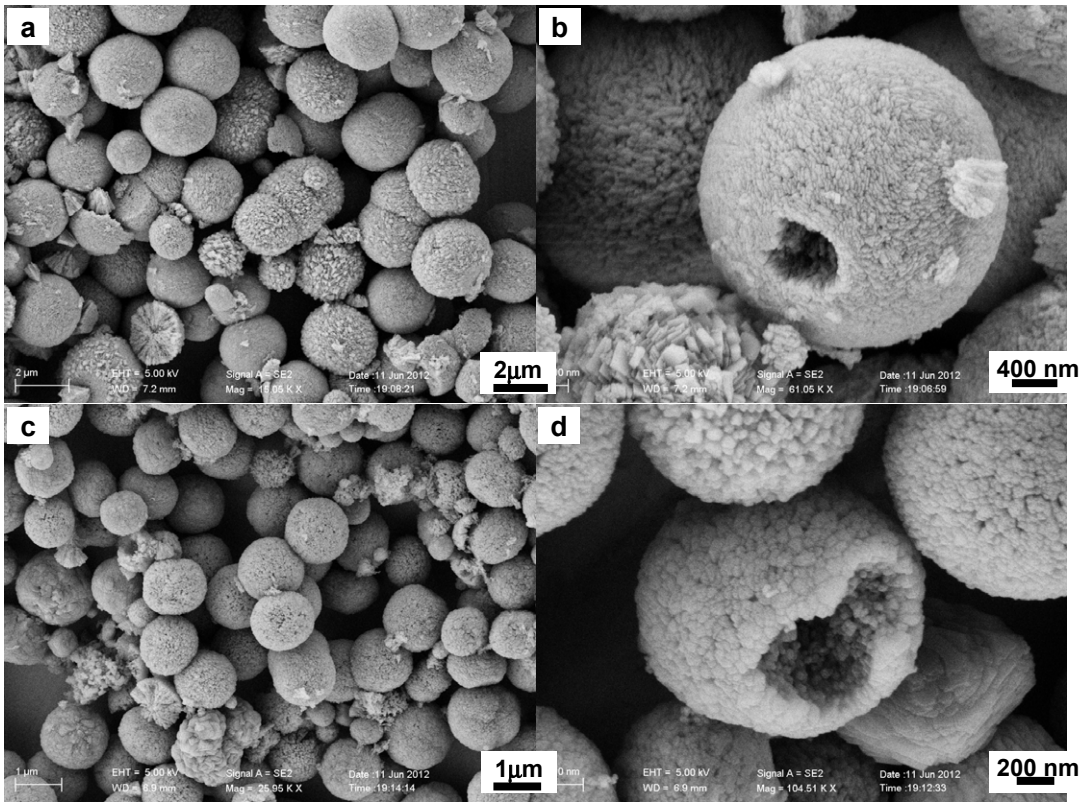

Figure S3. Low and high magnification FESEM images of the $Mn_{0.33}Co_{0.67}CO_3$ (a,b) and $Co_{0.33}Mn_{0.67}CO_3$ (c,d) precursors synthesized solvothermally at 220°C for 20 h.

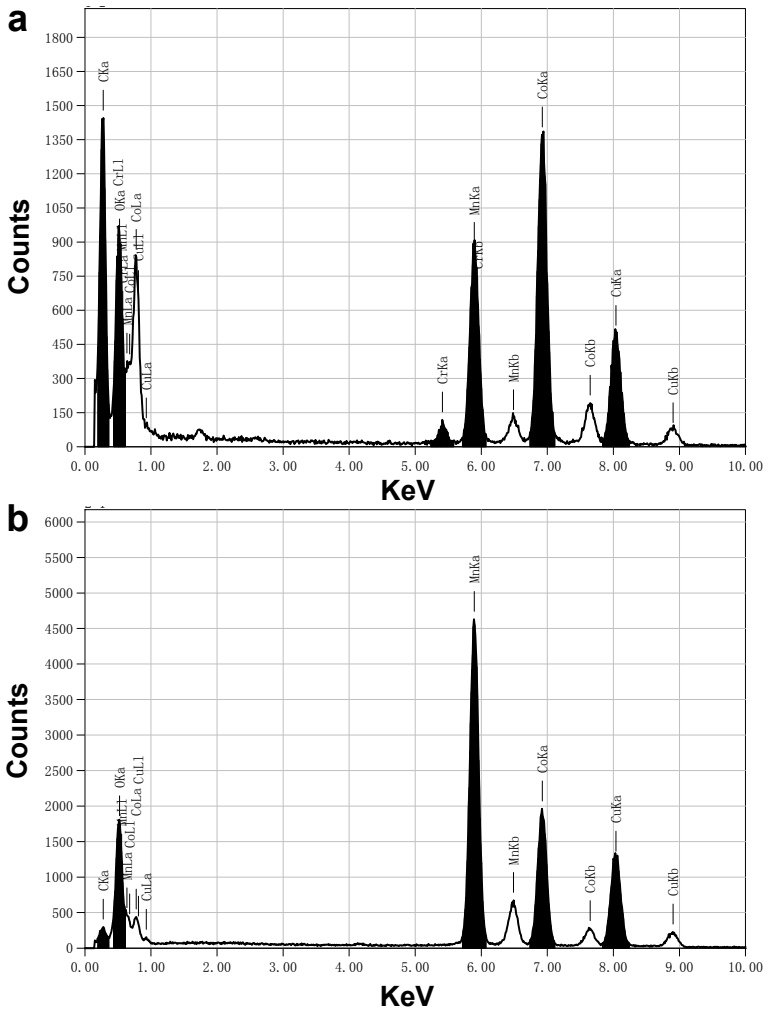

Figure S4. EDX spectrum of the $MnCo_2O_4$ (a) and $CoMn_2O_4$ (b) hollow microspheres.

Table S1. The ratio of Co(II)/Co(III) and Mn(II)/Mn(III) in the products based on the area of peaks after a Gaussian fitting method .

Composite	the ratio of Co(II)/Co(III)	the ratio of Mn(II)/Mn(III)	the ratio of O/M
$MnCo_2O_4$	0.81	1.70	1.36
$CoMn_2O_4$	2.30	0.36	1.51

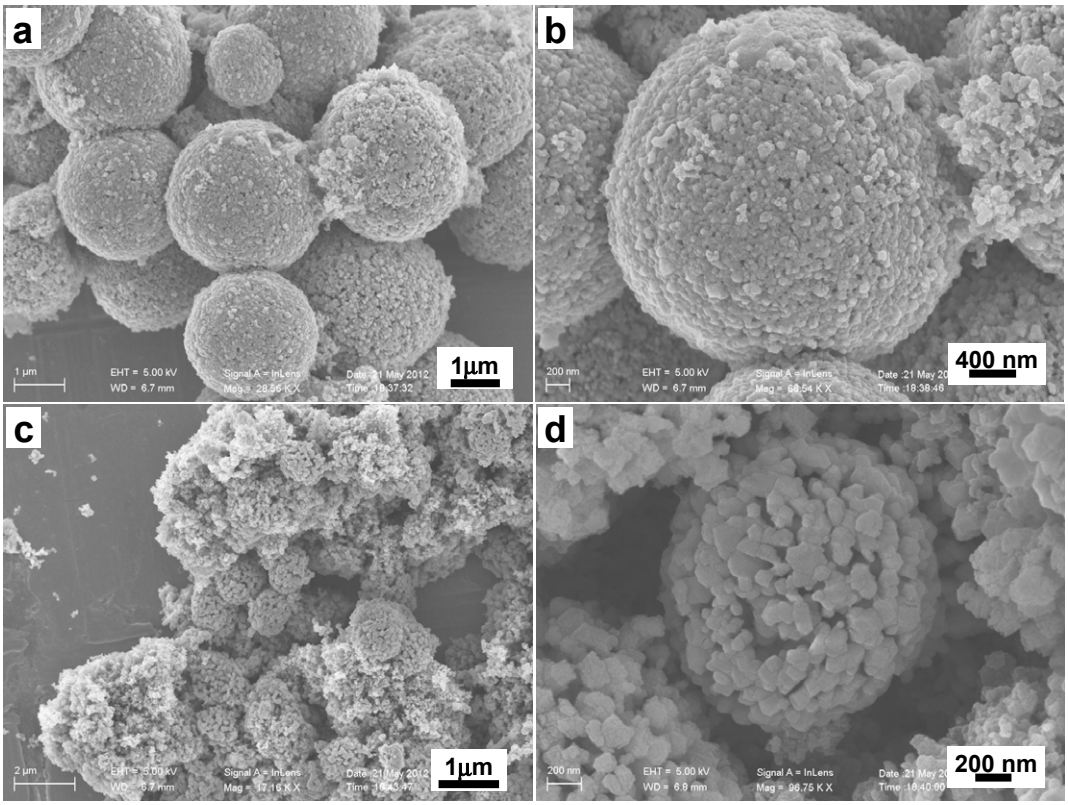

Figure S5. FESEM images of the electrode made of $MnCo_2O_4$ (a,b) and $CoMn_2O_4$ (c,d) after 100 cycles testing at 400 mA g^{-1}, respectively.

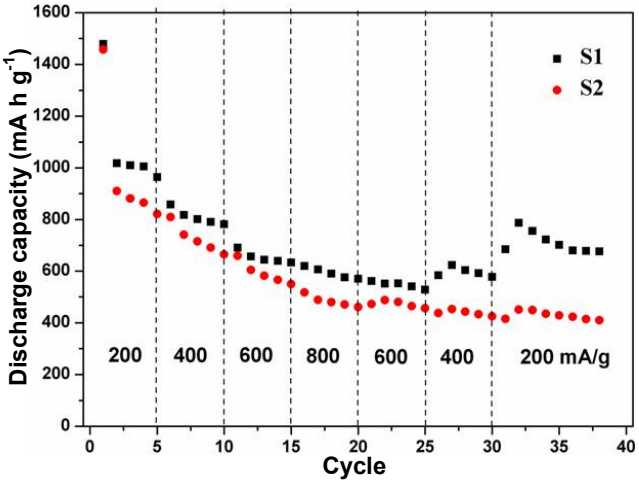

Figure S6. Rate performance of $MnCo_2O_4$ (S1) and $CoMn_2O_4$ (S2) electrodes.